Beyond superquenching: Hyper-efficient energy transfer from conjugated polymers to gold nanoparticles

Chunhai Fan*, Shu Wang*†, Janice W. Hong*†, Guillermo C. Bazan*†‡, Kevin W. Plaxco*†§, and Alan J. Heeger*‡¶‖

*Institute for Polymers and Organic Solids, Departments of †Chemistry and Biochemistry and ‡Materials, §Interdepartmental Biomolecular Science and Engineering Program, and ¶Department of Physics, University of California, Santa Barbara, CA 93106

Contributed by Alan J. Heeger, April 7, 2003

Gold nanoparticles quench the fluorescence of cationic polyfluorene with Stern–Volmer constants (K_{SV}) approaching 10^{11} M^{-1}, several orders of magnitude larger than any previously reported conjugated polymer–quencher pair and 9–10 orders of magnitude larger than small molecule dye–quencher pairs. The dependence of K_{SV} on ionic strength, charge and conjugation length of the polymer, and the dimensions (and thus optical properties) of the nanoparticles suggests that three factors account for this extraordinary efficiency: (*i*) amplification of the quenching via rapid internal energy or electron transfer, (*ii*) electrostatic interactions between the cationic polymer and anionic nanoparticles, and (*iii*) the ability of gold nanoparticles to quench via efficient energy transfer. As a result of this extraordinarily high K_{SV}, quenching can be observed even at subpicomolar concentrations of nanoparticles, suggesting that the combination of conjugated polymers with these nanomaterials can potentially lead to improved sensitivity in optical biosensors.

Water-soluble conjugated polymers have recently received attention as components in high-performance fluorescence sensor applications (1–5). The utility of these luminescent polyelectrolytes in biosensors originates from their high absorption coefficients (excellent ''light harvesters'') in combination with relatively high fluorescent quantum yields, and the extraordinarily efficient quenching of their luminescence emission by small molecule electron and energy acceptors (6, 7). For example, methyl viologen quenches the emission of poly[lithium 5-methoxy-2-(4-sulfobutoxy)-1,4-phenylenevinylene] (MBL-PPV) with a Stern–Volmer quenching constant (K_{SV}) of $\approx 10^7$ M^{-1} (1). This is 5–6 orders of magnitude more efficient than the quenching of typical small molecule dye–quencher pairs (8), an effect that translates into greatly improved sensitivity in fluorescence-based assays (1, 2). Were further increases in K_{SV} possible, they should thus translate directly into improved sensor performance.

The observation that gold metal efficiently quenches the emission of many fluorophores (9–11) suggests that gold nanoparticles might serve as efficient quenchers of conjugated polymer fluorescence. Huang and Murray (12) have described the quenching of small molecule dyes by gold nanoparticles, and Dubertret *et al.* (13) have elegantly used gold nanoparticles as an effective proximal quencher in DNA molecular beacons. The more general application of gold nanoparticles in sensor approaches, however, has been limited by relatively inefficient quenching of small molecule fluorophores; even the most effective small molecule dye–nanoparticle pairs yield $K_{SV} \approx 10^7$ M^{-1} (12). Here we describe conjugated polymer–gold nanoparticle pairs that, in contrast, exhibit K_{SV} approaching 10^{11} M^{-1}. This greatly increased K_{SV} provides insights into the mechanisms that underlie the extraordinarily efficient quenching of these materials. More interestingly, versatile chemistry available for surface functionization of gold nanoparticles (14) makes the gold nanomaterials especially suitable for possible ligand tethering and therefore applicable for use in high-performance conjugated polymer-based sensors (1).

Materials and Methods

The water-soluble conjugated polymers and oligomers seen in Scheme 1 were synthesized at the University of California, Santa Barbara as described (15–17). Gold nanoparticles were obtained from either Sigma (5, 10, or 20 nm) or British Biocell International, Cardiff, U.K. (2 nm). Concentrations of gold nanoparticles were adapted from the data provided by the manufacturer. Absorption spectra were collected with a Shimadzu UV-2401PC UV-visible recording spectrophotometer, and photoluminescence (PL) spectra were collected with a PTI fluorometer (Photon Technology International, Lawrenceville, NJ). The quartz cuvettes were treated by hexamethyldisilazane to block nonspecific electrostatic absorption of cationic polymers to anionic quartz surfaces (18). The fluorescence spectra were obtained by exciting poly(9,9′-bis(6-*N*,*N*,*N*-trimethylammonium)-hexyl)-fluorene phenylene (PF) at 375 nm, oligofluorene at 320 nm, poly(phenylene vinylene) at 480 nm, and phenyl vinylene oligomers at 400 nm. Reported K_{SV} and confidence intervals (Table 1) represent the mean and standard deviation of three independent measurements.

Results and Discussion

Stern–Volmer Quenching Measurements. Polyfluorenes are a family of blue-emitting conjugated polymers with large extinction coefficients and high PL quantum yields (19). Side-chain functionalization with quarternary amines renders polyfluorenes cationic and soluble in water. Here we have used cationic PF (Scheme 1). PF exhibits an intense blue emission, with major peaks at 417 and 440 nm.

The emission of PF is measurably quenched by 5-nm gold nanoparticles at subpicomolar concentrations. The K_{SV} is related to the PL efficiency via the relationship

$$\phi^\circ/\phi = 1 + K_{SV}[\text{quencher}], \qquad [1]$$

where ϕ° and ϕ are PL quantum efficiencies in the absence and presence of the quencher, respectively. A plot of ϕ°/ϕ vs. nanoparticle concentration demonstrates the highly efficient ''superquenching'' (15) produced by this fluorophore–quencher pair (Fig. 1). The plot is linear in the concentration range of 0 to 25 pM, with $K_{SV} = 8.3 \times 10^{10}$ M^{-1} (Table 1).

Evaluation of the K_{SV} Value. Linear Stern–Volmer plots provide a traditional and convenient means to determine K_{SV} values. Whitten and coworkers (20), however, have recently shown that

Abbreviations: PF, poly(9,9′-bis(6-*N*,*N*,*N*-trimethylammonium)-hexyl)-fluorene phenylene; PL, photoluminescence; K_{SV}, Stern–Volmer quenching constant; $(PRU/Q)_{50}$, polymer repeat units per quencher at 50% quenching; 2-OF, 2-oligofluorene; OPV, oligophenylene vinylene.

‖To whom correspondence should be addressed. E-mail: ajh@physics.ucsb.edu.

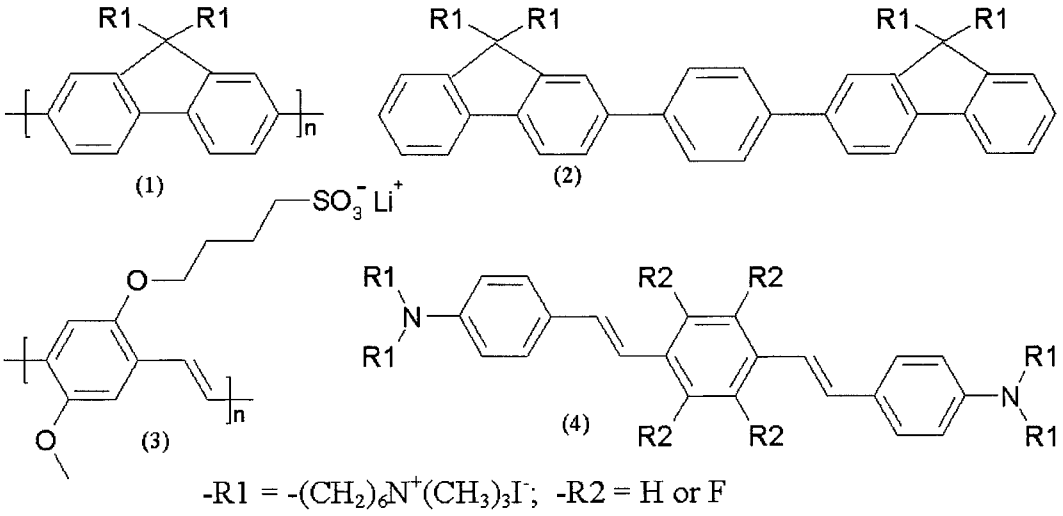

Scheme 1. Structure of **1**, PF; **2**, 2-OF; **3**, poly[lithium 5-methoxy-2-(4-sulfobutoxy)-1,4-phenylenevinylene] (MBL-PPV); and **4**, OPV-H and OPV-F.

K_{SV} values obtained in this way often depend on polymer concentration; i.e., K_{SV} is not truly constant. To avoid this difficulty, we have also calculated polymer repeat units per quencher at 50% quenching [$(PRU/Q)_{50}$], which, as demonstrated by Whitten and coworkers (21, 22), is a concentration-independent parameter. As illustrated (Table 1), the $(PRU/Q)_{50}$ values for polymers and oligomers described here closely follow the K_{SV} values obtained via more traditional, linear Stern–Volmer studies. For example, the $(PRU/Q)_{50}$ value for PF quenched by 5-nm gold nanoparticles is 1–2 orders of magnitude larger than the highest $(PRU/Q)_{50}$ value previously reported (22). Because K_{SV} values are widely used in the literature and are therefore effective for cross-comparison when the polymer concentration is held constant, we report K_{SV} values as an index of quenching efficiencies in the following studies.

The Quenching Mechanism. The superquenching of conjugated polymers by small molecule quenchers is thought to arise from efficient internal energy transfer or electron transfer within the polymer (6, 7) and the formation of static quenching complexes via attractive electrostatic interactions (1, 15, 23). Here we demonstrate that, in addition to these effects, long-range resonance energy transfer contributes significantly to the highly efficient quenching of PF by gold nanoparticles.

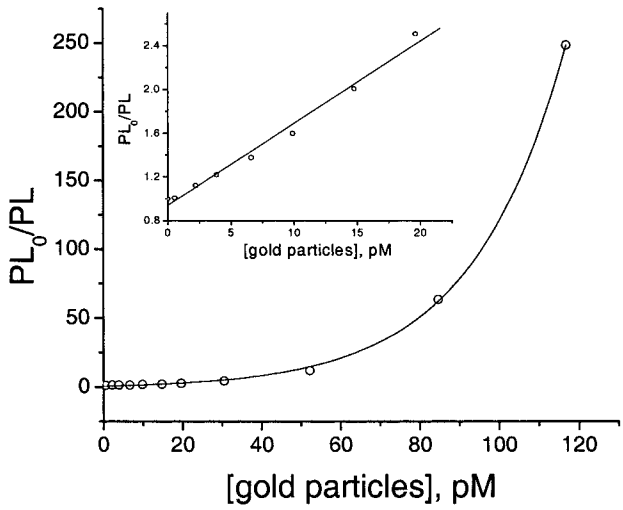

Fig. 1. Stern–Volmer plots of polyfluorene (1.0×10^{-6} M in monomer repeat units) quenching by 5-nm gold nanoparticles demonstrate the hyperefficient quenching of conjugated polymers by gold nanoparticles. (*Inset*) Linear range in the low quencher concentration regime.

Quenching Amplification via Internal Energy Transfer or Electron Transfer. Pairing gold nanoparticles with short fluorene oligomers characterized by a conjugation length of two repeat units [2-oligofluorene (2-OF); Scheme 1] yields $K_{SV} = 5.8 \times 10^9$ M^{-1} (Table 1). This order-of-magnitude reduction in quenching efficiency is consistent with the 10-fold difference in PF (the polymers contain ≈20 repeat units) and 2-OF conjugation length. Thus, the longer conjugation length of luminescent polymer (with respect to the oligomer) causes amplification of the quenching efficiency by gold nanoparticles. We ascribe this amplification to light harvesting by the high absorption coefficient of the conjugated polymer (a multichromophore system) followed by ultrafast internal excitation transfer to the site(s) closest to the quencher.

Internal excitation transfer via Förster resonant energy transfer requires good overlap between the emission of the light-harvesting chromophore and the absorption of the emitter. In the case of internal excitation transfer, the light-harvesting chromophore and the emitter are the same conjugated polymer chain. However, because of the relatively large Stokes shift typical of conjugated polymers, the overlap of the absorption and emission spectra obtained from conjugated polymers in solution is not large enough to support the ultrafast energy transfer implied by the superquenching data.

For the internal electron transfer mechanism, the intrachain electron mobility (μ) must be large enough to enable diffusion over the lengths of conjugated chains in the required subpicosecond regime. The diffusion length (L_D) along a one-dimensional chain in a time t_o is given by the following:

$$L_D \sim (Dt_o)^{1/2}, \qquad [2]$$

where D is the diffusion constant. Thus, with $t_o < 1$ ps and $L_D \approx 100$ Å, one concludes that $D > 1$. Using the Einstein relation, $\mu = eD/k_BT$, the implied mobility at room temperature is $\mu > 25$ $cm^2 \cdot V^{-1} \cdot s^{-1}$. Because the electron mobilities measured in semiconducting polymer films are at maximum $\mu \approx 0.1$ $cm^2 \cdot V^{-1} \cdot s^{-1}$, far too small to satisfy this criterion, the internal electron-transfer mechanism can be important only if

Table 1. K_{SV} and $(PRU/Q)_{50}$ of cationic polymers/oligomers quenched by gold nanoparticles

Polymer/ oligomer	Quenching efficiency	Gold nanoparticles			
		2 nm	5 nm	10 nm	20 nm
PF	K_{SV}	$\sim 10^7$	$8.3 \pm 0.8 \times 10^{10}$	$2.2 \pm 0.4 \times 10^{10}$	$7.8 \pm 0.5 \times 10^{10}$
	$(PRU/Q)_{50}$	<100	$8.5 \pm 0.2 \times 10^4$	$2.0 \pm 0.4 \times 10^4$	$7.3 \pm 0.4 \times 10^4$
2-OF	K_{SV}		$5.8 \pm 0.3 \times 10^9$		
	$(PRU/Q)_{50}$		$5.9 \pm 0.8 \times 10^3$		
OPV-H	K_{SV}		$7.8 \pm 0.4 \times 10^9$		
	$(PRU/Q)_{50}$		$7.3 \pm 0.2 \times 10^3$		
OPV-F	K_{SV}		$7.9 \pm 0.9 \times 10^9$		
	$(PRU/Q)_{50}$		$7.8 \pm 0.8 \times 10^3$		

the intrachain electron mobilities are $\mu > 25\ cm^2 \cdot V^{-1} \cdot s^{-1}$; i.e., much larger than the macroscopic mobilities measured, for example, in polymer-based field effect transistors (24). Measurements of the mobilities of isolated chains of semiconducting poly(phenylene vinylene) in solution yield mobilities of $0.2–0.5\ cm^2 \cdot V^{-1} \cdot s^{-1}$ (25). For semiconducting polymer chains in aqueous solution, there is evidence from small-angle neutron scattering of rigid rod behavior with long coherence lengths (26). Although such rigid rods could have somewhat higher mobility, $\mu > 25\ cm^2 \cdot V^{-1} \cdot s^{-1}$ is unlikely. Relatively little is known about the diffusion constant for exciton migration in semiconducting polymers, but internal excitation transfer via the diffusion of neutral excitons could also play a role. Thus, although both internal energy transfer and internal electron transfer within the elongated polymer chain have been suggested as the mechanism for the rapid internal excitation transfer, the mechanism remains unclear.

Electrostatic Complex Formation. Because of the adsorption of citrate during nanoparticle preparation, gold nanoparticles are typically negatively charged (27). As a result, static quenching is expected to arise from the strong Coulomb interaction between the anionic nanoparticles and the cationic polyfluorene (15, 28). Consistent with this hypothesis, even high concentrations of gold nanoparticles do not quench the anionic-conjugated polymer, poly[lithium 5-methoxy-2-(4-sulfobutoxy)-1,4-phenylenevinylene] (MBL-PPV) (Scheme 1 and data not shown). The quenching of short oligomers of cationic PPV polymers (Scheme 1), in contrast, is extremely efficient (Table 1).

Parallel studies by Whitten and coworkers (20) demonstrate that adsorption of small molecular dyes onto inert nanoparticles creates a "self-assembled polymer." The same effect may occur here. The formation of electrostatic complex between cationic polymers and gold nanoparticles may lead to a "polymer ensemble" in which a single gold nanoparticle can quench a large number of polymer chains. Such an effect would contribute to the extraordinary quenching efficiency that we observe.

Further evidence for the contribution of electrostatic complex formation is provided by the observation that increases in ionic strength significantly reduce quenching efficiency. We find that the emission of a largely quenched solution of 2-OF and gold nanoparticles (29) increases with the addition of salt until 90% recovery is observed at ionic strengths >0.6 M (Fig. 2). This finding is consistent with previous reports of reduced quenching efficiencies arising because of ionic screening; at high ionic strengths the debye screening length is sufficiently short that polymer–quencher complex formation is inhibited (28). Critically, these data also indicate that the binding energy of the complex is of order k_BT; thus, this quencher–polymer pair is suitable for use in conjugated polymer-based sensing applications in which complex formation must be readily reversible.

The presence of highly negatively charged gold nanoparticles might also alter the aggregation state of PF, an effect known to alter the fluorescence of other soluble conjugated polymers (1). As shown in Fig. 3, PF fluorescence quenching is accompanied by a small blue shift (several nanometers) in λ_{max}, suggesting that formation of the electrostatic complex increases polymer aggregation (1, 23). The blue shift is approximately the same as that observed for the parallel poly[lithium 5-methoxy-2-(4-sulfobutoxy)-1,4-phenylenevinylene] (MBL-PPV)/methyl viologen system, which is known to undergo quencher-induced aggregation and yet exhibits orders-of-magnitude-less-efficient quenching ($K_{SV} \approx 10^7$; ref. 1). Thus, PF aggregation cannot, by itself, account for the extraordinarily high K_{SV} we have observed.

Energy Transfer. A recent report suggests that both charge transfer and energy transfer play a role in quenching in fluorophore–gold particle nanoassemblies (30). We have investigated the roles that energy transfer and electron transfer play in the extremely efficient quenching reported here and find that, for gold nanoparticles of >2 nm, resonance energy transfer dominates the quenching mechanism.

As a probe of the quenching mechanism, we have determined K_{SV} for 2-, 10-, and 20-nm gold nanoparticles as quenchers. Both 10- and 20-nm gold nanoparticles quench the fluorescence of PF with efficiencies comparable with that of 5-nm nanoparticles (Table 1). Surprisingly, however, the K_{SV} of 2-nm gold nanoparticles is 4 orders of magnitude lower. This difference could arise

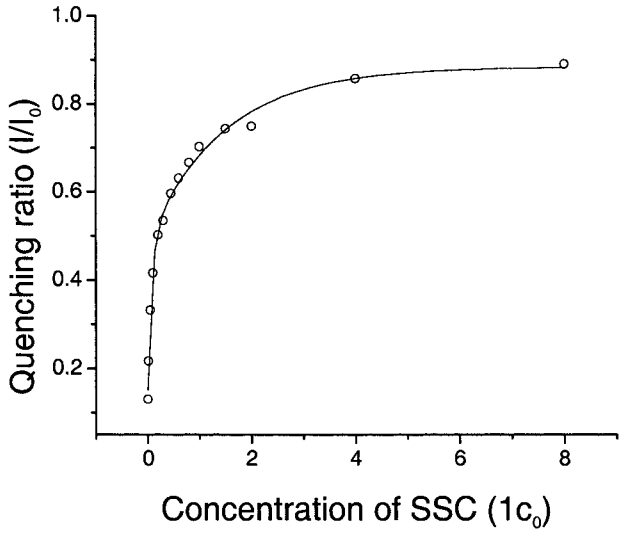

Fig. 2. The fluorescence quenching ratio of 2-OF is a sensitive function of ionic strength. The concentration of 2-OF is 1.0×10^{-6} M (in monomer repeat units) and that of the 5-nm gold nanoparticles is 3.4×10^{-10} M. The buffer concentration is in units of c_0: 1 c_0 of SSC buffer contains 0.015 M sodium citrate and 0.15 M NaCl, at pH 7.0.

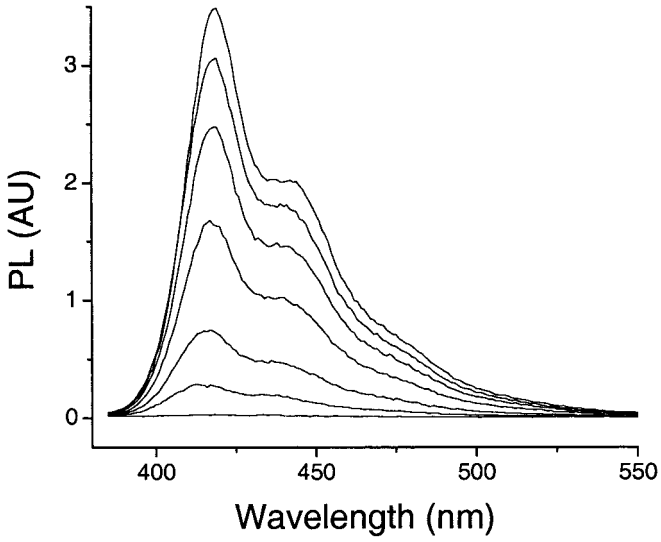

Fig. 3. Typical fluorescence spectra of polyfluorene (1.0×10^{-6} M in monomer repeat units) in the presence of 5-nm gold nanoparticles, with concentrations of 0, 2.2, 6.6, 15, 31, 52, and 120 pM (from top to bottom).

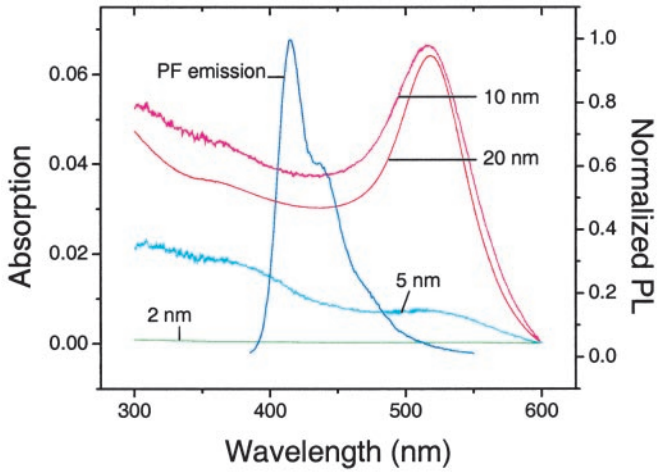

Fig. 4. The lack of significant overlap between the emission of PF and the absorbance of 2-nm nanoparticles implies that energy transfer between the two is not a significant quenching mechanism, thus accounting for the 4-orders-of-magnitude reduction in their K_{SV} relative to those of the larger nanoparticles. Shown are the absorption spectra of 2-, 5-, and 10-nm nanoparticles (at a concentration of 1 nM) and 20-nm nanoparticles (at a concentration of 0.1 nM). The absorption of 2-nm nanoparticles is 200-fold less than that of 5-nm nanoparticles and thus is invisible on this scale. Also shown is the fluorescence emission of polyfluorene (PF).

from the reduced surface area that would limit the polymer accommodation on the gold nanoparticles. Alternatively, we note that the impressive difference in the visible appearance of 2- and 5- to 20-nm gold nanoparticles parallels their quenching efficiencies: a solution of 2-nm nanoparticles is colorless, whereas solutions of the larger nanoparticles are intensely red. Spectroscopy confirms that, whereas 5- to 20-nm gold nanoparticles absorb strongly at 300–500 nm, the absorbance of 2-nm nanoparticles at these wavelengths is hundreds of times less intense (Fig. 4). Given that both PF and 2-OF emit at 400 nm, the absorptions of 5- to 20-nm gold nanoparticles overlap significantly with polymer emission, guaranteeing efficient energy transfer. Conversely, energy transfer between the polymer and 2-nm gold nanoparticles is not significant because of insufficient spectral overlap. This finding suggests that resonance energy transfer dominates the quenching observed for the larger gold nanoparticles.

The ability of 2-nm gold nanoparticles to quench polymer fluorescence despite their poor spectral overlap suggests that electron transfer may also contribute (although weakly) to the quenching. The 10,000-fold reduced K_{SV} of the 2-nm particles implies, however, that electron transfer is not the dominant quenching mechanism for the larger gold nanoparticles. This suggestion is further supported by studies of the quenching of cationic oligophenylene vinylene and a tetra-fluoro derivative (OPV-H and OPV-F, respectively; Scheme 1). Whereas the electronic structure of these conjugated oligomers differs significantly, thus leading to significantly differing electron transfer efficiencies, their emission features, and thus energy transfer efficiencies, are quite similar. The efficiencies with which 5-nm nanoparticles quench the fluorescence of these oligomers are, to within experimental error, indistinguishable (Table 1), providing additional support for the suggestion that resonance energy transfer, rather than electron transfer, dominates the quenching mechanism.

That quenching occurs via energy transfer rather than electron transfer may partially account for these extraordinarily high K_{SV} values. Whereas electron transfer is essentially a contact process (because of its exponential distance dependence), resonance energy transfer efficiency is high until quencher–fluorophore pair separation approaches the Förster radius. The Förster radius of fluoroscein–gold nanoparticle pairs has recently been measured at 6–8 nm (N. Reich and G. Strouse, personal communication). If the Förster radii of the gold nanoparticle-conjugated polymer pairs are similarly long, the ability of a single gold particle to quench many polymer molecules could contribute significantly to the efficiency of the quenching process.

Summary and Conclusion

With K_{SV} values approaching 10^{11} M^{-1}, the quenching of cationic-conjugated polymers by gold nanoparticles is several orders of magnitude more efficient than any previously reported conjugated polymer–quencher pair and 9–10 orders of magnitude more efficient than typical small molecule dye–quencher pairs. This hyperefficient quenching derives from three factors: (*i*) amplification of the quenching efficiency by energy transfer or electron transfer within the conjugated polymer; (*ii*) Coulombic interactions that ensure efficient binding of the conjugated polymer to the gold nanoparticles, leading to efficient static quenching; and (*iii*) the ability of gold to quench fluorescence via highly efficient, relatively long-range energy transfer. The electrostatically stabilized polymer–nanoparticle complex can be disrupted by ionic screening, indicating that quenching is a reversible process that should be readily adaptable to existing conjugated polymer-based biosensing platforms. Moreover, the hyperefficient quenching produced by these complexes should enable subpicomolar analyte detection.

This research was supported by National Science Foundation Grant NSF-DMR-0099843, Office of Naval Research Grant ONR N0014-1-1-0239, and National Institutes of Health Grant GM 62958-01.

1. Chen, L., McBranch, D. W., Wang, H., Helgeson, R., Wudl, F. & Whitten, D. G. (1999) *Proc. Natl. Acad. Sci. USA* **96,** 12287–12292.
2. Heeger, P. S. & Heeger, A. J. (1999) *Proc. Natl. Acad. Sci. USA* **96,** 12219–12221.
3. Gaylord, B. S., Heeger, A. J. & Bazan, G. C. (2002) *Proc. Natl. Acad. Sci. USA* **99,** 10954–10957.
4. Wang, D., Gong, X., Heeger, P. S., Rininsland, F., Bazan, G. C. & Heeger, A. J. (2002) *Proc. Natl. Acad. Sci. USA* **99,** 49–53.
5. Fan, C., Plaxco, K. W. & Heeger, A. J. (2002) *J. Am. Chem. Soc.* **124,** 5642–5643.
6. Swager, T. M. (1998) *Acc. Chem. Res.* **31,** 201–207.
7. Swager, T. M. & Wosnick, J. H. (2002) *MRS Bull.* **27,** 446–450.

8. Lakowicz, J. R. (1999) *Principles of Fluorescence Spectroscopy* (Kluwer, New York).
9. Pagnot, T., Barchiesi, D. & Tribillon, G. (1999) *Appl. Phys. Lett.* **75,** 4207–4209.
10. Kamat, P. V., Barazzouk, S. & Hotchandani, S. (2002) *Angew. Chem. Int. Ed. Engl.* **41,** 2764–2767.
11. Dulkeith, E., Morteani, A. C., Niedereichholz, T., Klar, T. A., Feldmann, J., Levi, S. A., van Veggel, F. C. J. M., Reinhoudt, D. N., Moller, M. & Gittins, D. I. (2002) *Phys. Rev. Lett.* **89,** 203002.
12. Huang, T. & Murray, R. W. (2002) *Langmuir* **18,** 7077–7081.
13. Dubertret, B., Calame, M. & Libchaber, A. J. (2001) *Nat. Biotechnol.* **19,** 365–370.
14. Gu, J. & Hacker, G. W. (2002) *Gold and Silver Staining: Techniques in Molecular Morphology* (CRC, Boca Raton, FL).
15. Wang, D., Wang, J., Moses, D., Bazan, G. C. & Heeger, A. J. (2001) *Langmuir* **17,** 1262–1266.
16. Stork, M., Gaylord, B. S., Heeger, A. J. & Bazan, G. C. (2002) *Adv. Mater.* **14,** 361–366.
17. Hong, J. W., Gaylord, B. S. & Bazan, G. C. (2002) *J. Am. Chem. Soc.* **124,** 11868–11869.
18. Wang, H., McBranch, D. W., Klimov, V. I., Helgeson, R. & Wudl, F. (1999) *Chem. Phys. Lett.* **315,** 173–180.
19. Leclerc, M. (2001) *J. Polym. Sci. Polym. Chem. Ed.* **39,** 2867–2873.
20. Jones, R. M., Lu, L., Helgeson, R., Bergstedt, T. S., McBranch, D. W. & Whitten, D. G. (2001) *Proc. Natl. Acad. Sci. USA* **98,** 14769–14772.
21. Lu, L., Jones, R. M., McBranch, D. & Whitten, D. (2002) *Langmuir* **18,** 7706–7713.
22. Lu, L., Helgeson, R., Jones, R. M., McBranch, D. & Whitten, D. (2002) *J. Am. Chem. Soc.* **124,** 483–488.
23. Tan, C. Y., Pinto, M. R. & Schanze, K. S. (2002) *Chem. Commun.*, 446–447.
24. Sirringhaus, H., Tessler, N. & Friend, R. H. (1998) *Science* **280,** 1741–1744.
25. Hoofman, R. J. O. M., de Haas, M. P., Siebbeles, L. D. A. & Warman, J. M. (1998) *Nature* **392,** 54–56.
26. Wang, D., Lal, J., Moses, D., Bazan, G. C. & Heeger, A. J. (2001) *Chem. Phys. Lett.* **348,** 411–415.
27. Templeton, A. C., Wuelfing, M. P. & Murray, R. W. (2000) *Acc. Chem. Res.* **33,** 27–36.
28. Wang, J., Wang, D., Miller, E. K., Moses, D., Bazan, G. C. & Heeger, A. J. (2000) *Macromolecules* **33,** 5153–5158.
29. Gaylord, B. S., Wang, S. J., Heeger, A. J. & Bazan, G. C. (2001) *J. Am. Chem. Soc.* **123,** 6417–6418.
30. Ipe, B. I., Thomas, K. G., Barazzouk, S., Hotchandani, S. & Kamat, P. V. (2002) *J. Phys. Chem.* **106,** 18–21.